N90-19410

1989

NASA/ASEE SUMMER FACULTY FELLOWSHIP PROGRAM

MARSHALL SPACE FLIGHT CENTER
THE UNIVERSITY OF ALABAMA IN HUNTSVILLE

MECHANICS OF AEOLIAN PROCESSES-

SOIL EROSION AND DUST PRODUCTION

Prepared by:	M. M. Mehrabadi, Ph.D.
Academic Rank:	Associate Professor
University and Department:	Tulane University Department of Mechanical engineering
NASA/MSFC Laboratory: Division: Branch:	 Space Science Laboratory Earth Science and Applications Division Fluid Dynamics
MSFC Colleague:	Nicholas C. Costes, Ph.D.
Date:	August 22, 1989
Contract No.:	The University of Alabama in Huntsville NGT-01-008-021

MECHANICS OF AEOLIAN PROCESSES- SOIL EROSION AND DUST PRODUCTION

by

M. M. Mehrabadi
Dept. of Mechanical Engineering
Tulane University
New Orleans, Louisiana 70118

ABSTRACT

Aeolian (wind) processes occur as a result of atmosphere / land-surface system interactions. A thorough understanding of these processes and their physical/mechanical characterization on a global scale is essential to monitoring global change and, hence, is imperative to the fundamental goal of the Earth Observing System (Eos) program.

Soil erosion and dust production by wind are of consequence mainly in arid and semi arid regions which cover 36% of the Earth's land surface. Some recent models of dust production due to wind erosion of agricultural soils and the mechanics of wind erosion in deserts are reviewed and the difficulties of modeling the aeolian transport are discussed in this report.

ACKNOWLEDGMENTS

The financial support of the NASA/ASEE Summer Faculty Program is gratefully acknowledged. The author is indebted to Drs. N. C. Costes (NASA/MSFC), Goudarz Ahmadi (Clarkson University), Bruce White (University of California, Davis), Robert S. Anderson (University of California, Santa Cruz), Dale A. Gillette (National Oceanic and Atmospheric Administration), Ayo Oyediran (NRC), and Yemo Fashiola (UAH) for stimulating discussions of their publications on this subject matter.

FIGURE CAPTIONS

FIG. 1 Major deserts of the world and directions and distances of dust transport (after Pewe, 1981)

FIG. 2 Major paths of airborne soil dust from West Africa and North Africa (from Rapp, 1977, after Pewe, 1981)

FIG. 3 Log-height vs. wind speed profiles for deriving the hypothetical wind speed $U(z_r)$ at reference height z_r (with reference roughness height z_{or}) from the wind speed $U(z_s)$ measured at station height z_s (with effective upwind roughness height z_{os}) (redrawn from Wieringa, 1976)

FIG. 4 Vertical flux of dust (g cm^{-2} s^{-1}) as a function of friction velocity (cm s^{-1}) (after Gillette and Passi, 1988)

FIG. 5 Schematic representation of modes of aeolian transport (from Kind, 1989)

FIG. 6 Differential intensity of bombardment on windward and lee slopes (after Bagnold, 1941)

FIG. 7 Coincidence of ripple wavelength and range of characteristic path of grain (after Bagnold, 1941)

FIG. 8 Coefficient A as a function of the threshold particle friction Reynolds number, B (after White, 1986)

FIG. 9 Schematic diagram showing the trajectory of a particle.

FIG. 10 Saltation trajectories (after White, 1986)

MECHANICS OF AEOLIAN PROCESSES - SOIL EROSION AND DUST PRODUCTION

1. INTRODUCTION

Aeolian (wind) processes occur as a result of atmosphere/land-surface system interaction. Study of this interaction is one of the broad geologic science issues identified by the Earth Observing System (Eos) Science and Mission Requirement Group (Butler et al., 1984) and the Eos Science Steering Committee (Butler et al., 1987). A fundamental goal of Eos is to develop an improved understanding of the processes that control the formation and evolution of the solid Earth. Aeolian processes are persistent sculptors of the face of the planet Earth (and Mars). Hence a thorough understanding of these processes and their physical/chemical characterization is essential to monitoring global change and, thus, is imperative to this goal.

Wind erosion and transport are active geologic processes that occur mainly in arid and semi-arid regions which cover 36% of the Earth's land surface. Arid and semi-arid areas suffering from "desertification" undergo destruction of native vegetation which is quickly followed by an excessive soil erosion. Examples of areas with severe soil erosion are northern China, including part of the Loess Plateau and Inner Mongolia, the Thar desert of eastern Pakistan and northwest India, and the U.S. Great Plains, including parts of Texas, Oklahoma, and New Mexico.

Although soil erosion by wind is of consequence mainly in arid and semi-arid regions, it may occur wherever soil, vegetation, and climatic conditions are conducive. Generally, wind erosion is effective when soil is loose, fine, and dry, and has little or no vegetation. The present rate of fertile soil loss in the United States may be as high as 100 tons per acre per year in half a dozen major agricultural regions, including the corn-belt states of Iowa, Missouri and Illinois. The Council on Environmental Quality (Sheridan, 1981) estimates that about 10 percent of the U.S. land mass is in a state of severe or very severe desertification.

Large dust storms originate in major deserts of the world (Fig. 1). In most of these deserts, dust is formed by in situ weathering of bedrock and from abrasion of the bedrock by the wind-blown sand (Goudie, 1978). Large,

frequent dust storms originate from normally semi-arid areas (e.g., the Great Plains of the United States; Central India; and the Russian steppes) that periodically become arid, undergo abnormally strong windy periods, or have their vegetation removed by man or nature (Pewe, 1981).

In terms of particle size, dust can be divided into two major groups depending on how far a distance they can be transported by the wind (Pewe, 1981). Dust particles that are carried between a few kilometers to less than 100 km, by dust devils and dust storms, are mostly between 0.005 mm to 0.05 mm. The other type of dust consists of particles between 0.002 mm and 0.01 mm in size. This fine-grained, sorted dust is carried to the troposphere as an aerosol (i.e., a dust that remains suspended in the air until brought down by rainfall onto water and land surfaces). Dust from the Sahara collected in the Caribbean (Fig.2) has been reported to be more than 98% smaller than 0.01 mm (Prospero, et al., 1970).

Aerosols affect the reflectance, transmittance and absorptance of the atmosphere (Verstraete, et al., 1988). They modify the amount of shortwave radiation absorbed and longwave radiation emitted by the climatic system. Their impact on the climate is further enhanced by their role as cloud condensation nuclei.

Aerosols impact on the transfer of radiation through the atmosphere also affects the interpretation of the satellite remote sensing data. While this creates a nuisance for data obtained using passive remote sensing techniques, aerosols provide excellent tracers when active instruments such as the Laser Atmospheric Wind Sounder (LAWS) are used for wind velocity measurements.

Dust has many other serious environmental consequences. These include its effect on crop growth, ocean sedimentation and its effect on the acid/base balance of atmospheric deposition. Dust storms cause disease, suffocation of cattle, development of static electricity, disruption of transportation, and destruction of property.

A model for the estimation of total dust production for the United States has been discussed recently by Gillette (1988). After reviewing this model in Sec. 3, the mechanics of aeolian transport of particulate materials is discussed in Sec. 4. The long and short term goals of this research effort are described in the next section.

2. OBJECTIVES

Some recent literature on mechanical modeling of aeolian processes are reviewed in this report. Specifically, two kinds of models are discussed. The first kind deals with the agricultural soil erosion and dust production by wind. The second kind deals with the more basic problem of wind erosion in deserts.

This effort is part of a comprehensive program of research focused on assessing the potential impact of desertification on climate changes and global habitability. The ultimate goal of this research is to develop a quantitative understanding of the mechanics of atmospheric coupling with land systems, as related to desert processes in arid and semi-arid regions. Existing data banks, data generated by laboratory experimentation and, later, data generated by Eos sensors will be used in the validation stage of the model.

The short term goal of this research is the formulation and validation of a model for the main mechanisms involved in the aeolian transport of particles based on principles of mechanics at the particle-scale. At present, no comprehensive quantitative analysis of such processes is available.

3. A MODEL FOR DUST EMISSION BY WIND EROSION

A model for the total dust production for the United States, recently proposed by Gillette and Passi (1988), is reviewed in this section. The primary use of the model is in the inventory of alkaline elements for use in acid/base balance studies of atmospheric precipitation by the National Acid Precipitation Assessment Program (NAPAP).

3.1 Wind Profile in the Lower Planetary Boundary Layer

In the atmospheric inertial sublayer, which is the lower part of the planetary boundary layer, the wind speed can be assumed to vary with height according to the logarithmic wind profile (see, e.g., Priestely, 1959, or Plate, 1971)

$$U(z) = \frac{V_*}{0.4} \ln \frac{z}{z_o} \qquad (3.1)$$

if the stratification is nearly adiabatic (for winds above the velocity required for wind erosion of soils, Gillette, 1981, reported that the atmosphere was neutrally stratified). In (3.1), z_o denotes atmospheric roughness height, taken to be 1 cm for smooth surfaces (e.g., airport surfaces), and V_* is the friction velocity defined in terms of the shearing stress (shearing force per unit area of ground surface parallel to the wind direction) as

$$V_* = \sqrt{\frac{\tau}{\rho}} \qquad \text{or} \qquad \tau = \rho V_*^2 \qquad (3.2)$$

where ρ is the air density. Note that V_* is the velocity of the wind at a height approximately equal to 1.492 z_o .

It is convenient sometimes to introduce a drag coefficient, C_d , defined by (Priestely, 1959)

$$C_d \equiv \frac{\tau}{\rho U^2} = \left(\frac{V_*}{U}\right)^2 \qquad (3.3)$$

where $(3.3)_1$ has been written using $(3.2)_1$ to eliminate τ. Gillette and Passi (1988) use a method proposed by Wieringa (1976) to evaluate the drag coefficient C_d . This procedure is summarized in the next two paragraphs.

Wieringa (1976) takes the wind speed at a height of z_b = 60 m to be regionally constant. In other words, he assumes that the wind speed at that height, $U(z_b)$, does not show excessively the influence of the particular roughness element close to the wind station where an average wind speed $U(z_s)$ is measured at a height z_s. Suppose that at the same location we wish to know the average wind speed $U(z_r)$ over a hypothetical flat open reference terrain at a height z_r. Referring to Fig. 3, and calculating the slopes of the two wind profiles, will give

$$\frac{\ln z_b/z_s}{U(z_b) - U(z_s)} = \frac{\ln z_s/z_{os}}{U(z_s)} \qquad (3.4)$$

and

$$\frac{\ln z_b/z_r}{U(z_b) - U(z_r)} = \frac{\ln z_r/z_{or}}{U(z_r)} \qquad (3.5)$$

Eliminating $U(z_b)$ between (3.4) and (3.5), one finds

$$U(z_r) = U(z_s) \frac{\ln z_b/z_{os} \ln z_r/z_{or}}{\ln z_s/z_{os} \ln z_b/z_{or}} \qquad (3.6)$$

This is the required relation between $U(z_r)$ and $U(z_s)$.

If z_r is taken to be 1.492 z_{or}, so that $\ln z_r/z_{or}$ = 0.4, then from (3.1) it follows that $U(z_r) = V_*$ and from (3.6) it follows that

$$V_* = U(z_s) \frac{0.4 \ln z_b/z_{os}}{\ln z_s/z_{os} \ln z_b/z_{or}} \qquad (3.7)$$

Using (3.7), the drag coefficient can be calculated from (3.3) as

$$C_d = \left[\frac{0.4 \ln z_b/z_{os}}{\ln z_s/z_{os} \ln z_b/z_{or}} \right]^2 \qquad (3.8)$$

Gillette and Passi (1988), use a value for z_{os} = 1 cm, typical of clipped grass at airports, and z_{or} = 0.002 cm, from an average measured aerodynamic roughness heights they obtained in many experiments. With these values they find that

$$C_d = \left(\frac{0.23}{\ln z_s} \right)^2 \qquad (3.9)$$

where z_s is in cm. Substitution of (3.9) in (3.3) yields

$$V_* = \frac{0.23}{\ln z_s} U \qquad (3.10)$$

which relates the friction velocity to the wind speed.

3.2 Threshold Friction Velocity

Threshold friction velocity for wind erosion corresponds to the minimum wind stress needed to overcome forces holding soil particles in place. Threshold friction velocity is denoted by V_{*t} and is defined in terms of surface shear stress at threshold (or "threshold wind stress"), τ_t, by the relations

$$V_{*t} = \sqrt{\frac{\tau_t}{\rho}} \qquad \text{or} \qquad \tau_t = \rho V_{*t}^2 \qquad (3.11)$$

Although one must rely heavily on the values of the threshold friction velocity for estimation of dust production and wind erosion, there exists no theory for relating this quantity to the physical characteristics of the soil.

Threshold friction velocity has been determined experimentally for idealized surfaces by many investigators (see Gillette, 1988, for references) starting with the pioneering work of Bagnold (1941) who proposed a formula for V_{*t} in terms of the particle diameter and density (see section 4.1 of this report). The physical circumstances in agricultural soils is complicated, however, because of a wide variety of particle sizes and the effects of wetting/drying, freezing/thawing, vegetation, and aggregation of particles. Measurements of the threshold friction velocities for dust production for a wide class of agricultural soils has been reported only recently by Gil-

lette (1988). Gillette and Passi's estimation of dust production is based on the measurements of Gillette (1988) and the values of threshold friction velocity obtained for arid regions by Gillette et al. (1980, 1982).

3.3 Dust Flux as a Function of Wind Speed

Figure 4 shows the vertical flux of dust, G (g $cm^{-2} s^{-1}$) as a function friction velocity. The data were reported by Gillette (1974,1981) who measured dust fluxes in outdoor eroding fields, Fairchild and Tillery (1982) and Borrman and Jaenicke (1987), who measured fluxes with indoor wind tunnels.

Gillette and Passi (1988) express the flux of dust, G, by the relation

$$G = C_1 V_*^4 \left(1 - \frac{V_{*t}}{V_*}\right) \qquad (3.12)$$

where C_1 is a constant. This is shown as curve A in the Figure. Gillette and Passi (1988), state that (3.12) is based on an unpublished theory of Owen (personal communication between Gillette and Owen, 1987).

Substituting from (3.10) into (3.12), gives

$$G(U) = C_1 \left(\frac{0.23}{\ln z_s}\right)^4 U^4 \left(1 - \frac{U_t}{U}\right) \qquad (3.13)$$

where U_t is the threshold wind velocity obtained from (3.10), i.e.,

$$V_{*t} = \frac{0.23}{\ln z_s} U_t \qquad (3.14)$$

Let p(U) be the probability density function of the wind speed during the time period of interest. A widely used probability density function for natural winds is the two-parameter Weibull distribution (Gillette and Passi, 1988)

$$p(U) = \frac{k}{c}\left(\frac{U}{c}\right)^{k-1} e^{-(U/c)^k} \qquad (3.15)$$

where the two parameters c and k are determined directly from the wind data. The data set used by Gillette and Passi (1988), "the Wind Energy Resource Information System (WERIS)", provided monthly values of the mean hourly wind speed and the "pattern factor" statistics

$$x = \frac{\overline{U^3}}{\overline{U}^3} \tag{3.16}$$

where a bar over a quantity indicates the mean of the quantity for each month. WERIS provided data for a 31-year period, 1948-1978, for 1432 wind measuring locations in the United States. It turns out that the pattern factor x is a unique function of Weibull shape parameter, k, so that

$$x = \frac{\Gamma(1+3/k)}{\Gamma^3(1+1/k)} \tag{3.17}$$

where Γ is the gamma function. Given x, (3.17) can be solved for k by trial and error.

With the probability density function of the wind speed p(U), given by (3.15), G(U) is integrated for all wind speeds above the threshold, U_t for each location (subarea) of the region of interest, i.e.,

$$\bar{G}(U_t) = \int_{U_t}^{\infty} G(U)\, p(U)\, dU \tag{3.18}$$

$$= C_1 \left(\frac{0.23}{\ln z_s}\right)^4 \frac{k}{c} \int_{U_t}^{\infty} U^4 \left(1 - \frac{U_t}{U}\right) \left(\frac{U}{c}\right)^{k-1} e^{-(U/c)^k} dU$$

where $\bar{G}(U_t)$ is the average value of the flux estimates, G(U), for one sub-area, and where (3.13) and (3.15) are used to write (3.18) .

3.4 Estimation of Total Dust

The region of interest is divided into N sub-areas. Then the average value of the flux estimate for each sub-area $\bar{G}(U_t)$ (mass per unit area per unit time) is calculated from (3.18). This averaged estimates are then summed over all erosion areas within the region of interest, using various parameters as weighting function. Thus the mass of dust, E, emitted in the time period ΔT is written as (Gillette and Passi, 1988)

$$E = C \sum_{i=1}^{N} R_i \, g(L_i) \, A_i \, \bar{G}(U_{t_i}) \, \Delta T \qquad (3.19)$$

where C is a constant to be determined by calibration (the constant C_1 coming from G is lumped into C); i is the index of summation over N different erodible areas within the region of interest; R_i is the effect of soil roughness; $g(L_i)$ is the effect of field length, L_i; A_i is the area of the land being considered.

Roughness of the soil has the effect of trapping soil particles, increasing the friction velocity of the wind and thus inhibiting erosion. For this reason the exact effect of soil roughness is complicated. Gillette and passi (1988) examined data from the U.S. Department of Agriculture 1982 National Resource Inventory (NRI) for soil information, land use, and wind erosion parameters to evaluate a "ridge roughness function" proposed by Armbrust et al. (1964) which was based on wind tunnel tests. Since over 97% of these values examined in the data set were between 0.5 and 1 (for prominent erosion areas located largely in the panhandles of Texas and Oklahoma), they conclude that the maximum effect on dust production can not be more than a factor of 2.

The effect of field length on dust production is thought to be (Gillette and Passi, 1988) (i) an aerodynamic feedback mechanism whereby the airborne sand increase the aerodynamic roughness height by absorbing forward momentum from the wind and thus decreasing its speed, and (ii) an increase of soil flux with increasing field length due to sandblasting of the loosened downwind soils. Gillette and Passi (1988) assume $g(L_i)$ to be 1, ignoring the effect of change with distance downwind of the dust flux. It should be noted that mechanisms

similar to those described in (i) and (ii) are incorporated in a recent numerical model considered by Anderson and Haff (1988).

To evaluate C in equation (3.19), Gillette and Passi (1988) make use of data from total dust production for a large area including the panhandles of Texas and Oklahoma. They find a value of 1.4×10^{-15} for the constant C.

4. AEOLIAN TRANSPORT OF SAND IN DESERTS

A major contribution to the study of the physics of wind-blown sand in deserts was made by the classic work of Bagnold (1941) who combined extensive in-situ observations and wind-tunnel experiments to describe the motion of sand particles in the air.

Transport of dust, sand and other particulate materials by wind takes place mainly in the form of surface creep, saltation, and suspension (Bagnold, 1941). Surface creep, also known as "traction" is the movement of particles along the surface. Saltation refers to a leaping motion of particles where they lift off the surface and travel in ballistic-type trajectories in the air before returning to the surface. Suspension is the motion of (less massive) particles that are carried upwards by the wind to travel at indefinite heights within atmosphere (Fig. 5).

Bagnold (1941) states that of the total sand in motion in air about three-fourths move in saltation and a quarter in surface creep. The surface creep consists of slow jerky advance of the surface grains which are knocked along the surface by the impact of descending saltating grains. According to Bagnold, a saltation of fine grains can maintain a surface creep over a bed composed of grains far too large to be moved by the direct action of the wind.

Bagnold notes that a flat sand surface is inherently unstable. He argues that since the grains are of varying size, the surface is not perfectly even and tiny depressions can form such as the one shown, much magnified, in Fig. 6. The series of parallel lines shown in the figure are supposed to represent the descending saltating grains. On the lee side, along the line AB, the points of impact are far apart, but on the windward side many impacts occur. This means that the original depression will get bigger. Eventually, grains accumulate at C and a second lee slope CD is formed, and so on. Using this line of reasoning, Bagnold explains the formation of ripples and argues that the range of the characteristic path of grains is coincident with the ripple wavelength (Fig. 7).

Since saltation is the main mechanism of aeolian transport in sand, the remainder of this section is devoted to a review of some recent works on this topic (White, 1986, Anderson and Hallet, 1986).

4.1 Threshold Conditions

Bagnold (1941) has shown that at the initiation of saltation, the surface shear stress at threshold is

$$\tau_t = A^2 (\rho_p - \rho) g D_p \qquad (4.1)$$

where A is a varying empirical coefficient, ρ_p is the particle density, g is the acceleration due to gravity, and D_p is the mean particle diameter. In terms of the friction speed at threshold, V_{*t},

$$V_{*t} = A \sqrt{\frac{(\rho_p - \rho) g D_p}{\rho}} \qquad (4.2)$$

Since the particle density (2.64 g/cm^3 for quartz) is much greater than the atmospheric air density (1.22 x 10^{-3}) we have

$$\frac{\rho_p}{\rho} \simeq 2164 >> 1 \qquad (4.3)$$

Thus (4.2) can be written as

$$V_{*t} = A \sqrt{\frac{\rho_p g D_p}{\rho}} \qquad (4.4)$$

Bagnold and others have shown that A = A(B), where

$$B = \frac{V_{*t} D_p}{\nu} \qquad (4.5)$$

is the particle friction Reynolds number. In (4.5), ν is the kinetic viscosity of air. The variation of A with B obtained from wind tunnel data is shown in Fig. 8 (after White, 1979). Note that A $\simeq$ 0.118 for values of B > 10.

4.2 Forces acting on the Particle

Forces acting on the particle are (i) body force which results from gravity, $\underset{\sim}{F}_G$, (ii) aerodynamic drag, $\underset{\sim}{F}_D$, (iii) aerodynamic lift, $\underset{\sim}{F}_L$, and (iv) Magnus lift which results from particle spin, $\underset{\sim}{F}_M$. The trajectory of a typical saltating is schematically represented in Fig. 9. Note that a number of forces including the foce due to buoyancy (since $\rho \ll \rho_p$) and the interparticle force have been neglected; see White (1986) for a detailed discussion of these and other forces.

Aerodynamic drag is a function of the velocity of the particle relative to the air, $\underset{\sim}{V}_{rel}$,

$$\underset{\sim}{V}_{rel} = \underset{\sim}{U} - \underset{\sim}{U}_p \qquad (4.6)$$

where $\underset{\sim}{U}_p$ (with components $\dot{x}$ and $\dot{z}$) is the particle velocity. The drag force is expressed as

$$\underset{\sim}{F}_D = \frac{1}{2} C_D \left(\frac{\pi D_p^2}{4} \right) \rho \, V_{rel} \underset{\sim}{V}_{rel} \qquad (4.7)$$

where C_D is the drag coefficient which is a function of the particle Reynolds number, $Re = V_{rel} D_p / \nu$, i.e.,

$$C_D = C_D (Re) \qquad (4.8)$$

Aerodynamic lift is due to shear flow and its magnitude is given by (see Anderson and Hallet, 1986)

$$F_L = \frac{1}{2} C_L \left(\frac{\pi D_p^2}{4} \right) \rho \left(U_{top}^2 - U_{bot}^2 \right) \qquad (4.9)$$

where U_{top} and U_{bott} are the air speeds, at heights corresponding to the top and bottom of the grain, and C_L is given by (Chepil, 1958)

$$C_L = 0.85 C_D \qquad (4.10)$$

The Magnus lift is given by (see White, 1986, and Anderson and Hallet, 1986)

$$\underset{\sim}{F}_M = \frac{1}{8}\left(\frac{\pi D_p^3}{8}\right)\left(\underset{\sim}{\Omega} \times \underset{\sim}{V}_{rel}\right) \qquad (4.11)$$

where $\underset{\sim}{\Omega}$ is the angular velocity of the particle.

Rubinow and Keller (1961) derived the following relations for the moment, M, on a particle due to its spin Ω,

$$M = \mu\left(\pi D_p^3\right)\left(\frac{1}{2}\frac{\partial U}{\partial z} - \Omega\right) \qquad (4.12)$$

where μ is the air viscosity. Given the forces and the moment acting on the particle, equations of motion for the particle can be written and a numerical solution for the particle trajectories can be obtained (see White, 1986, and Anderson and Hallet, 1986).

4.3 Saltation Trajectories

Given a liftoff angle, α, speed of liftoff U_{p0}, and initial particle spin, Ω_0, the particle trajectory is numerically obtained using time iterations. At each time step, the Reynolds number is calculated, a drag coefficient is found, and the spin rate and local shear are calculated. Using these, accelerations, velocities, and displacements are updated for each increment. Results obtained by White (1986) are shown in Fig. 10.

5. CONCLUSIONS AND RECOMMENDATIONS

Some recent models of dust production due to wind erosion of agricultural soils (Gillette and Passi, 1988) and mechanics of wind erosion in deserts (Bagnold, 1941, and others) were reviewed in sections 3 and 4 of this report. It can be seen that in spite of the progress made so far, there are several issues that need more attention.

Within the framework of the models described two specific issues should be addressed as a next step (i) modeling of the threshold velocity particularly for agricultural soils, relating it to texture, moisture, etc., and (ii) the initiation of saltation which is still a source of controversy. The actual mechanism of particle liftoff and the forces operating at the initial stage are not well understood. The recent work of Anderson and Haff (1988) seem to be promising in this regard.

More generally, however, there are several viewpoints for modeling of particle-gas flows, namely, the "discrete particle" or "tracking" approach (see, for example, Durst, et al., 1981) and the "non-discrete" or continuum approach (see Ahmadi, 1986). The suitability of these approaches for modeling aeolian transport of soils must be examined in detail. The most significant aspect of the problem is modeling the interaction between the air-particle mixture and the boundaries of the flow. There is a continuous exchange of mass, momentum and energy between the bed and the air-particle system. Unless we take these exchanges into account, using basic principles, we have to rely on empirical formulas for dealing with wind erosion and dust production problems.

6. REFERENCES

Ahmadi, G. (1982), "A Continuum Theory for Two Phase Media," Acta Mechanica, 44, 299.

Anderson, R.S., and Hallet, B. (1986), "Sediment Transport by Wind: Toward a General Model," Geol. Soc. America Bull., 97.

Anderson, R.S., and Haff, P.K. (1988), "Simulation of Eolian Saltation," Science, 24, August.

Armbrust, D.W., Chepil, W., and Siddowway, F. (1964), "Effects of Ridges on Erosion of Soil by Wind," Soil Sci. Soc. Am. Proc. 28.

Bagnold, R. A. (1941), The Physics of Blown Sand and Desert Dunes, Methuen, London.

Borrman, S., and Jaenicke, R. (1987), "Wind Tunnel Experiments on the Resuspension of Sub-micrometer Particle From a Sand Surface," Atmos. Environ., 21, 1891-1898.

Butler, D., et al. (1984), Earth Observing System: Science and Mission Requirements Working Group Report, Vol I, NASA TM 86129.

Butler, D., et al. (1987), From Pattern to Process: The Strategy of the Earth Observing System, Report of the Eos Science Steering Committee, Vol. II.

Chepil, W.S. (1958), "The Use of Evenly Spaced Hemispheres to Evaluate Aerodynamic Forces on a Soil Surface," Trans., American Geophysical Union, 39, 3.

Durst, F., et al. (1984), "Eulerian and Lagrangian Predictions of Particulate Two-Phase Flows: A Numerical Study," Appl. Math. Modelling, 8.

Fairchild, C.I., and Tillery, M.I. (1982), "Wind Tunnel Measurements of the Resuspension of Ideal Particles," Atmos. Environ, 16.

Gillette, D.A. (1974), "On the Production of Soil Wind Erosion Aerosols Having the Potential for Long Range Transport," J. Rech. Atmos., 8.

Gillette, D.A., et al. (1980), "Threshold Velocities for Input of Soil Particles Into the Air by Desert Soils," J. Geophys. Res., 85.

Gillette, D.A. (1981), "Production of Dust That Can Be Carried Great Distances," Geol. Soc. Am., 186.

Gillette, D.A., et al. (1982), " Threshold Friction Velocities and Rupture Moduli for Crusted Desert Soils for the Input of Soil Particles into the Air," J. Geophys. Res. 87.

Gillette, D.A. (1988), "Threshold Friction velocities for Dust Production for agricultural Soils," J. Geophys. Res.

Gillette, D.A., and Passi, R. (1988), "Modeling Dust Emission by Wind Erosion," J. Geophys. Res., 93.

Goudi, A.S. (1978), "Dust Storms and Their Geomorphological Implications," J. of Arid Environ., 1.

Kind, R.J. (1989), "Mechanics of Aeolian Transport of Snow and Sand," Proc. 6th U.S. Nat. Conf. on Wind Eng., U. of Houston, Houston, Texas.

Pewe, T.L. (1981), Desert Dust: Origin, Characteristics, and Effect on Man, Geol. Soc. Am. 186.

Plate, E.J. (1971), Aerodynamic Characteristics of Atmospheric Boundary Layer, U.S. Atomic Energy Commission, Office of Information Services.

Priestley, C.H.B., Turbulent Transfer in the Lower Atmosphere, University of Chicago Press, Chicago.

Prospero, J.M., et al. (1970), " Dust in the Caribbean Atmosphere Traced to an African Dust Storm," Earth and Planetary Science Letters, 9.

Sheridan, D., Desertification of the United States, Council on Environmental Quality; Superintendent of Documents, U.S. Government Printing Office, Washington, D.C.

Verstraete, M.M., et al., (1988) "The NASA/EOS Aerosol Project," NCAR Ms. 8076/88-4.

White, B.R. (1979), "Soil Transport by Winds on Mars," J. Geophys. Res., 84.

White, B.R. (1986), "Particle Dynamics in Two-Phase Flows," Encyclopedia of fluid Mechanics, Gulf Publishing Co. Houston, Texas.

Wieringa, J. (1976), "An Objective Exposure Correction Method for Average Wind Speeds Measured at a Sheltered Location," Q. J. R. Meteorol. Soc., 102.

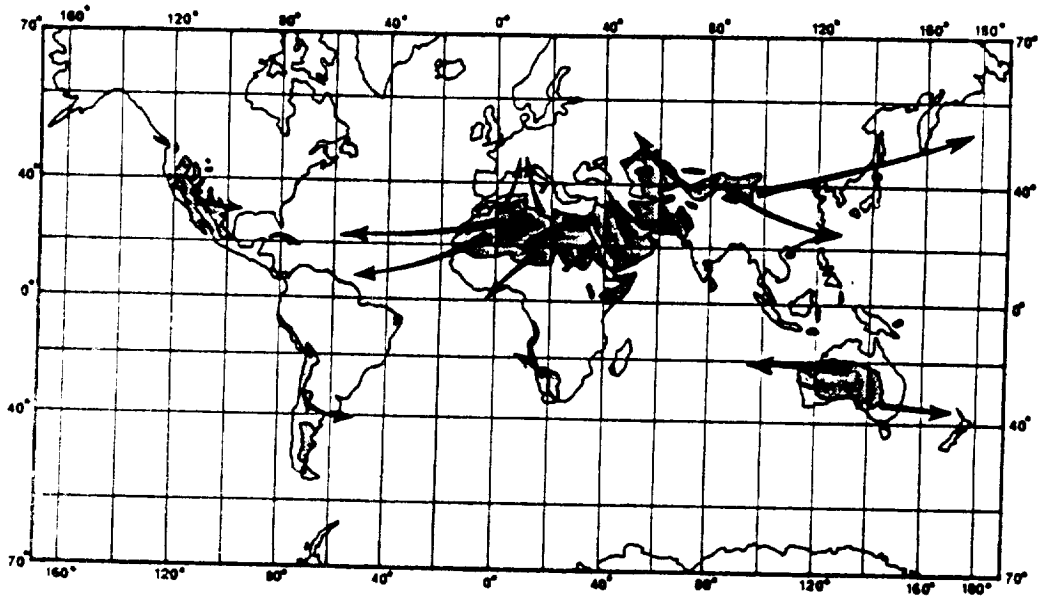

FIG. 1

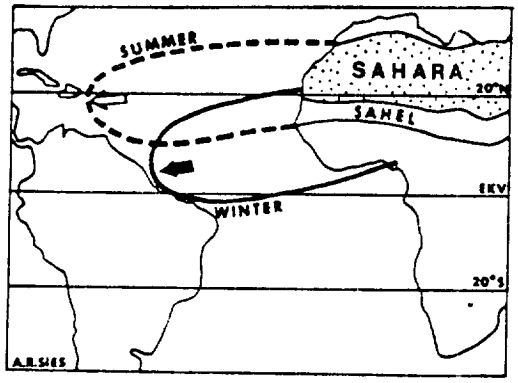

FIG. 2

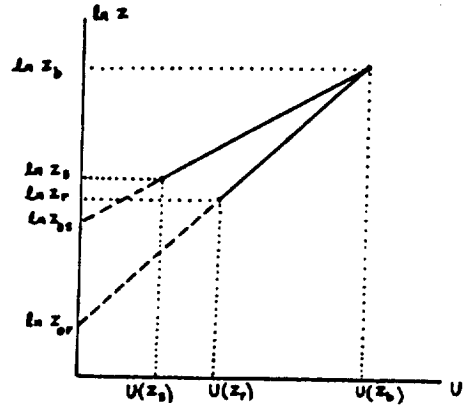

FIG. 3

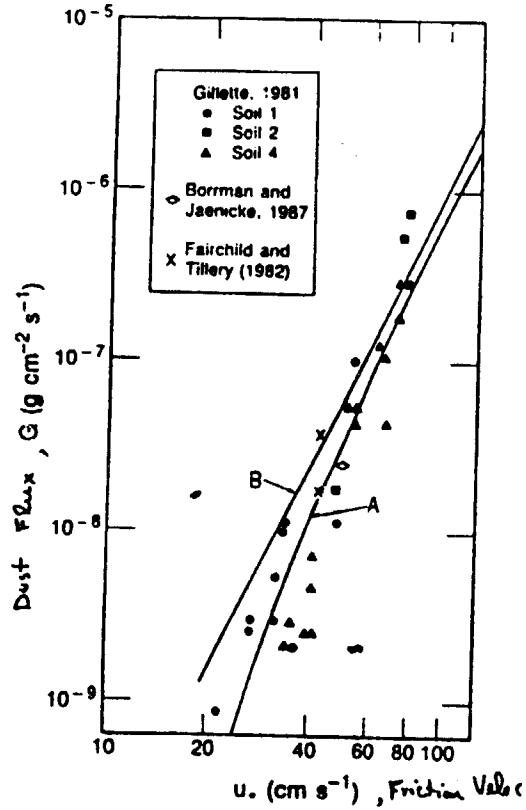

FIG. 4

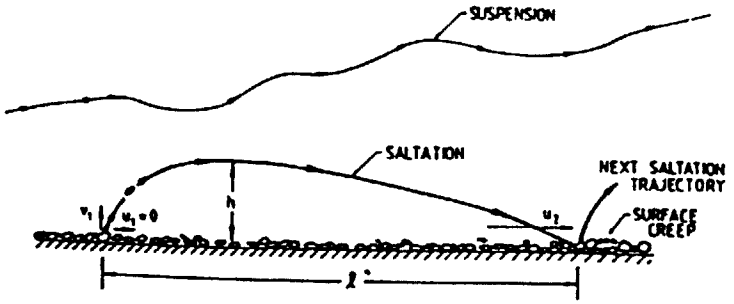

FIG. 5

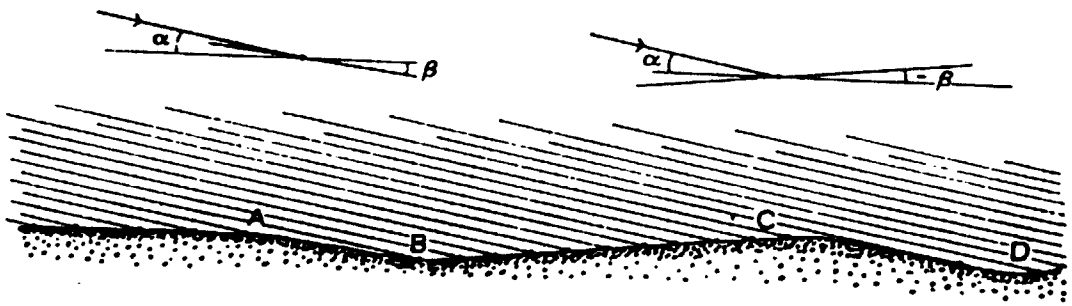

FIG. 6

FIG. 7

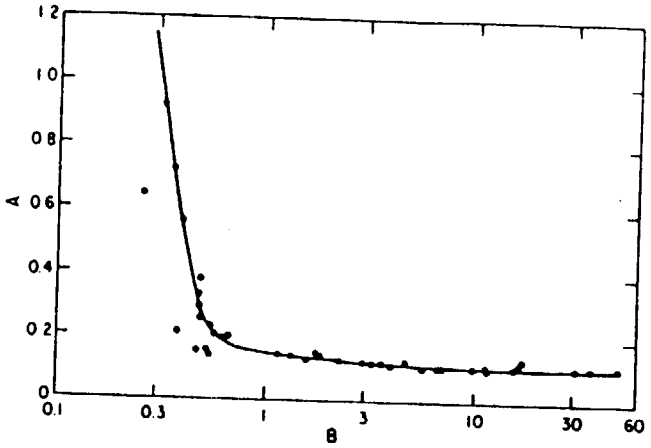

FIG. 8

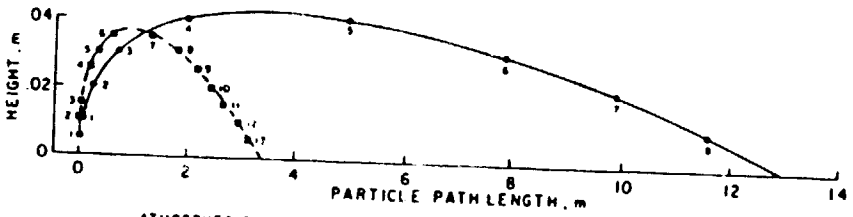

ATMOSPHERIC PRESSURE CASE

POSITION	VELOCITY, m/sec	PERCENT, U_∞
1	2.6	10
2	4.7	18
3	7.2	28
4	12.6	49
5	15.4	60
6	18.8	73
7	22.1	90
8	23.1	90
9	23.5	91
10	23.6	91
11	23.7	92
12	23.7	92
13	23.5	91

LOW PRESSURE CASE

VELOCITY, m/sec	PERCENT, U_∞
5.3	5.3
12.9	12.9
22.6	22.6
37.3	37.3
53.2	53.2
61.8	61.8
65.7	65.7
67.6	67.6

FIG. 10

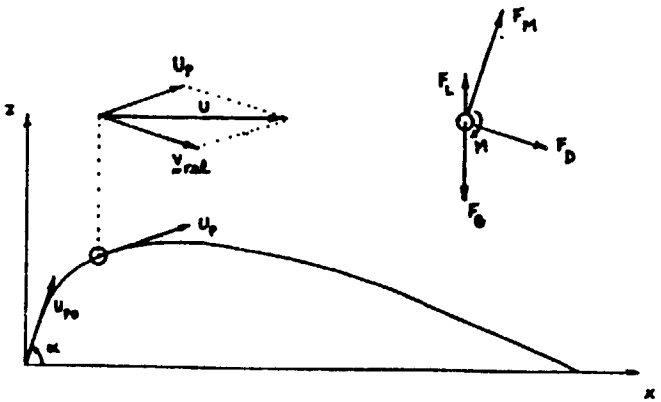

FIG. 9